Supporting Information for

Rapid fabrication of optical elements for sensing applications using a standard SLA printer

María Amparo Hernández-García, Knut Rurack, Jérémy Bell

Bundesanstalt für Materialforschung und -prüfung, Richard-Willstätter-Str. 11, 12489 Berlin, Germany

Table of content

I.	Printed optical elements	S2
II.	Laser scanning microscope imaging for surface roughness calculation	S7
III.	Post-treatment	S10
IV.	Front-face excitation-emission matrices	S12
V.	Environmental stability	S13
VI.	Refractive indexes	S14
VII.	Sensors	S15

I. Printed optical elements

a)

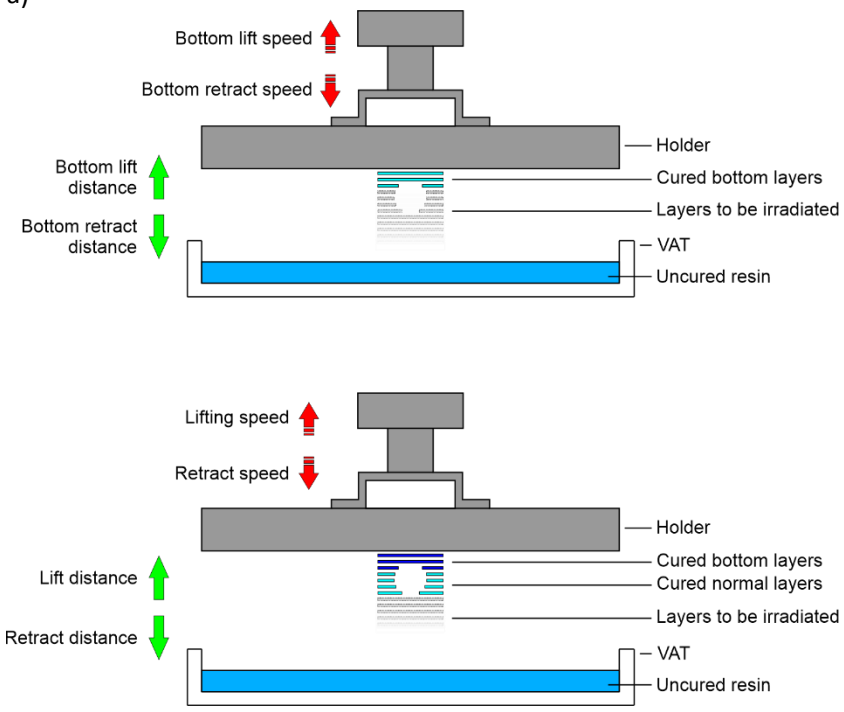

b)

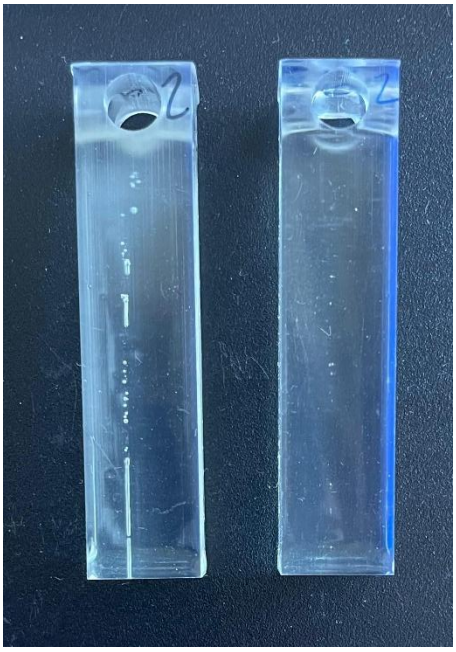

Figure S1. a) Cross section scheme of the printer when preparing bottom layers (top) and when adding normal layers (bottom) with irradiation through the VAT bottom, indicating the speeds and distances relevant for process control. b) Two rectangular cuboid blocks fabricated with **resin 1**, with lifting distance of 6 mm, lifting speed of 60 mm min^{-1} and retract speed of 150 mm min^{-1} (left) and with lifting distance of 5 mm, lifting speed of 50 mm min^{-1} and retract speed of 140 mm min^{-1} (right) (identical bottom and normal layer values).

Table S1. List of printing parameters

Parameter	Layers	Action	Influence on printing	Typical values (clear resins)	Custom values
Bottom lift distance	Bottom	How far the build plate moves upward to separate the cured layers from the vat film	Larger distances ensure better adhesion to the plate and separation from the film but prolong duration. Distances that are too short carry the risk of the layers sticking together or peeling off	5–8 mm	5 mm
Lifting distance	Normal				
Bottom retract distance	Bottom	The distance by which the build plate moves back into resin after being lifted	Controls how well the resin flows back under the build platform. Gaps that are too small can lead to incomplete curing	5–8 mm	5 mm
Retract distance	Normal				
Bottom lift speed	Bottom	The speed at which the build plate lifts during the growth of the bottom layers, where the adhesive forces are highest	Higher speeds accelerate the printing process but can lead to distortions and errors. Lower speeds reduce stress and improve reliability but increase printing time	40–60 mm min^{-1}	50 mm min^{-1}
Lifting speed	Normal	The lifting speed of for normal layers, typically faster than the bottom lift speed		80–120 mm min^{-1}	
Bottom retract speed	Bottom	The downward speed for the build plate	Higher speeds shorten cycle times, but excessive speeds can trap air, disrupt resin flow, or result in weak layers. Lower speeds allow for uniform resin reflow and ensure strong adhesion	100–150 mm min^{-1}	140 mm min^{-1}
Retract speed	Normal			150–200 mm min^{-1}	

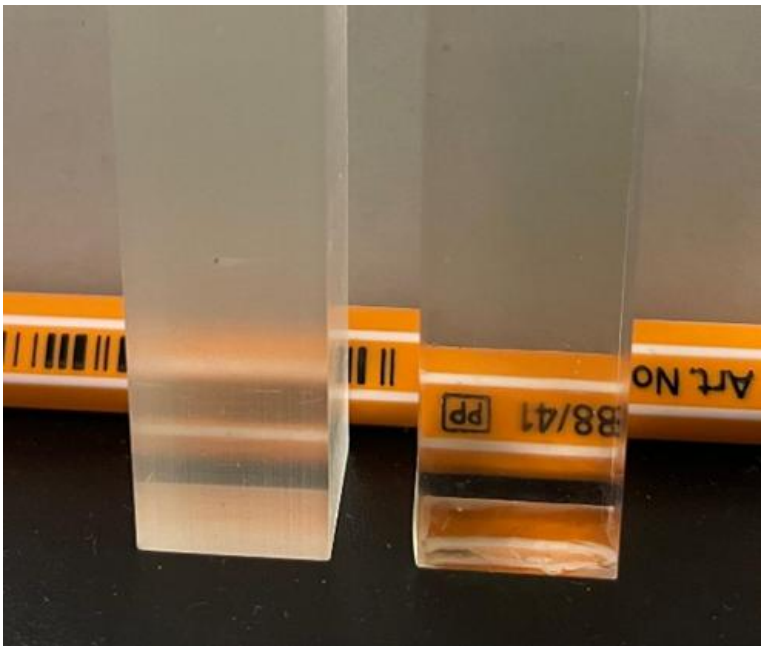

Figure S2. Two rectangular cuboid blocks fabricated with **resin 1**, without post-treatment (left) and with post-treatment (right).

Table S2. Deviation from theoretical thickness, height, diameter, and radius of curvature of a manufactured set of 5 rectangular cuboid "cuvette-like" blocks of 12.4 × 12.4 × 55 mm and a set of 10 plano-convex lenses (LA1951, Thorlabs) manufactured from **resin 1** after post-treatment.

Element	***Cuboid***	***Plano-convex lens***		
Parameter	Thickness* (mm)	Thickness* (mm)	Diameter* (mm)	Radius of curvature** (mm)
Design	12.400	11.700	25.400	13.100
Commercial	-	11.810	25.360	13.172
Deviation	-	0.110	0.040	0.072
Manufactured	14.378	11.446	25.547	13.071
Deviation	0.022	0.154	0.147	0.029

** Measurement error of 10 µm*
*** Measurement error of 50 µm*

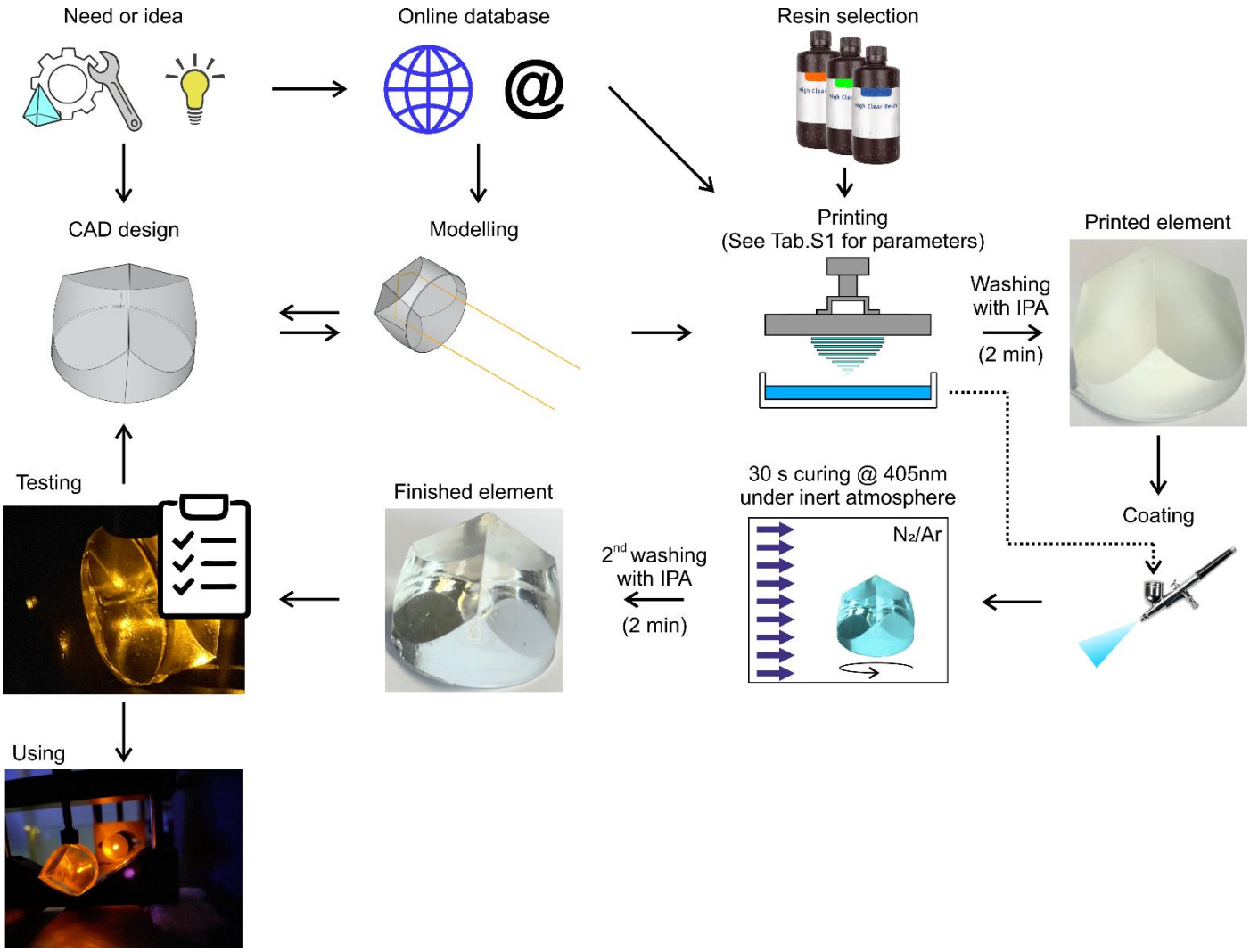

Figure S3. Optimal process for rapid prototyping of an optical element made from **resin 1**, from the need or idea to the finished element, including modelling and testing of the element for possible geometry adjustments. The given parameters are optimal for **resin 1** when printed on a Phrozen 8k Mini SLA printer and cured with a wash and cure machine 2.0 from Anycubic.

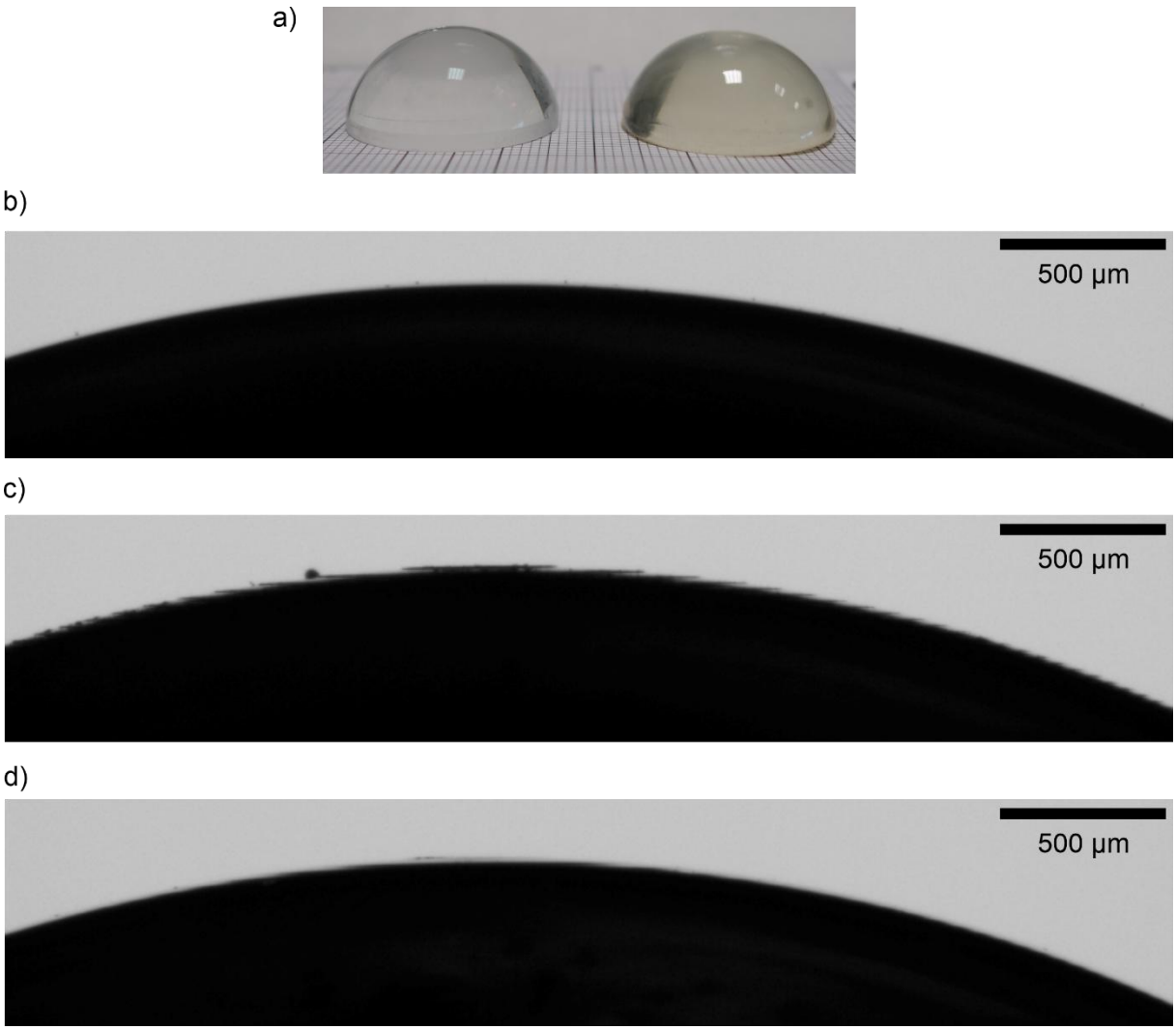

Figure S4. a) Photograph of plano-convex lenses (Ø = 25.4 mm) made from NBK-7 (left) obtained from the manufacturer (LA1951, Thorlabs) and manufactured with **resin 1** (right), following the method developed here. Profiles of b) a commercial NBK-7 lens and of a manufactured lens with **resin 1** c) without post-treatment and d) with post-treatment.

II. Laser scanning microscope imaging for surface roughness calculation

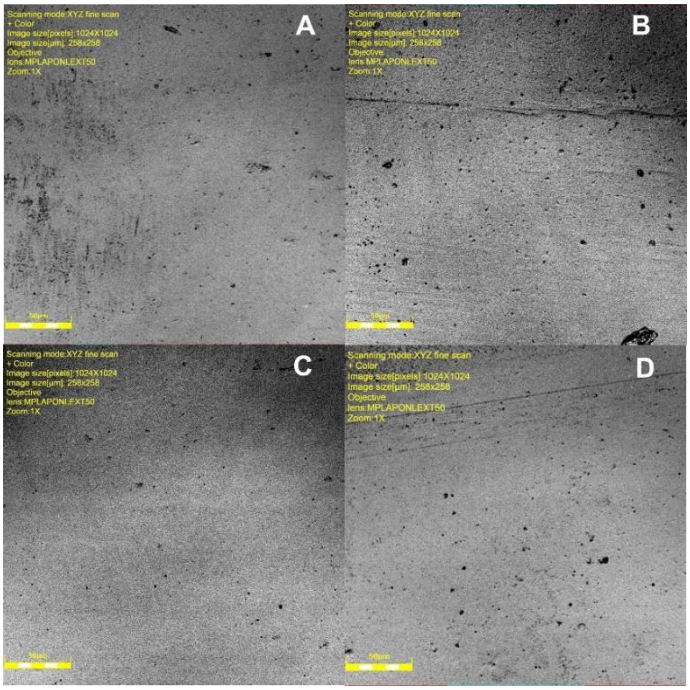

Figure S5. Laser scanning images (258 × 258 µm), with nominal magnification of x50, of four different points of a 3D printed rectangular cuboid block with **resin 1** in which the described post-treatment has been applied.

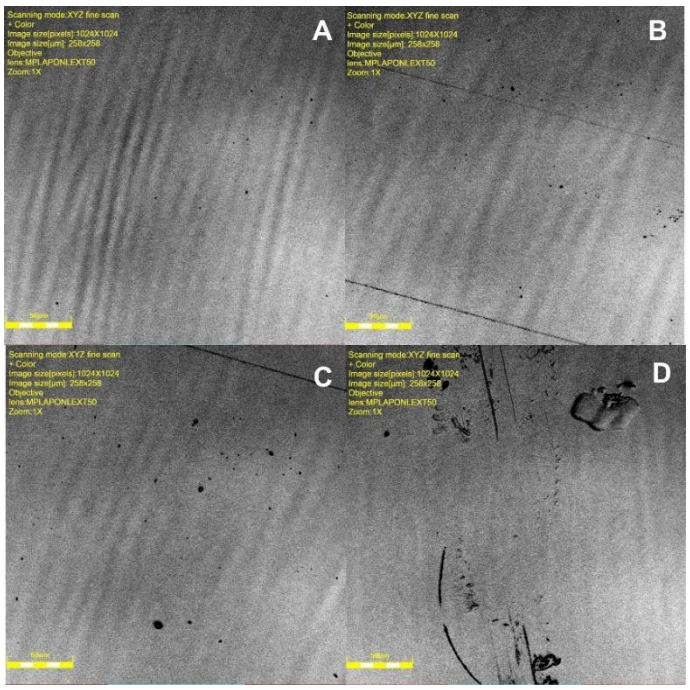

Figure S6. Laser scanning images (258 × 258 µm), with nominal magnification of x50, of four different points of a 3D printed rectangular cuboid block with **resin 2** in which the described post-treatment has been applied.

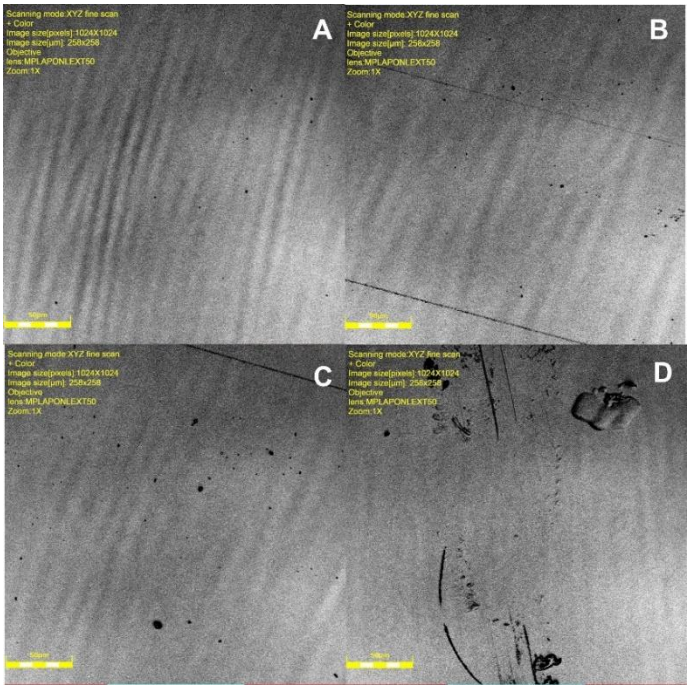

Figure S7. Laser scanning images (258 × 258 µm), with nominal magnification of x50, of four different points of a 3D printed rectangular cuboid block with **resin 3** in which the described post-treatment has been applied.

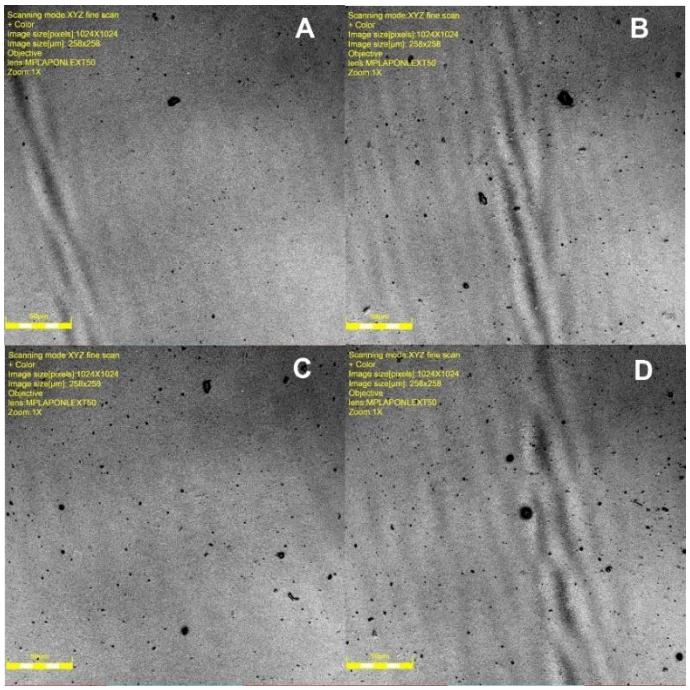

Figure S8. Laser scanning images (258 × 258 µm), with nominal magnification of x50, of four different points of a 3D printed rectangular cuboid block with **resin 5** in which the described post-treatment has been applied.

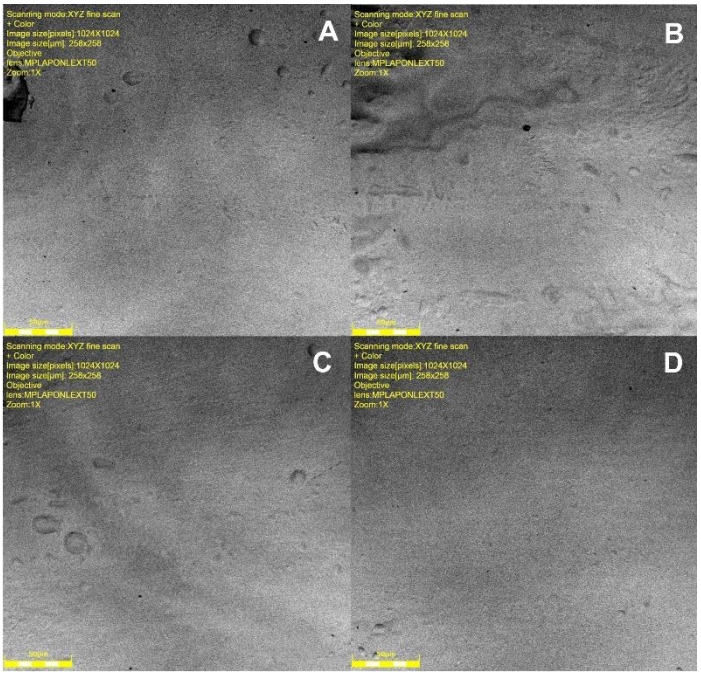

Figure S9. Laser scanning images (258 × 258 µm), with nominal magnification of x50, of four different points of a 3D printed rectangular cuboid block with **resin 6** in which the described post-treatment has been applied

III. Post-treatment

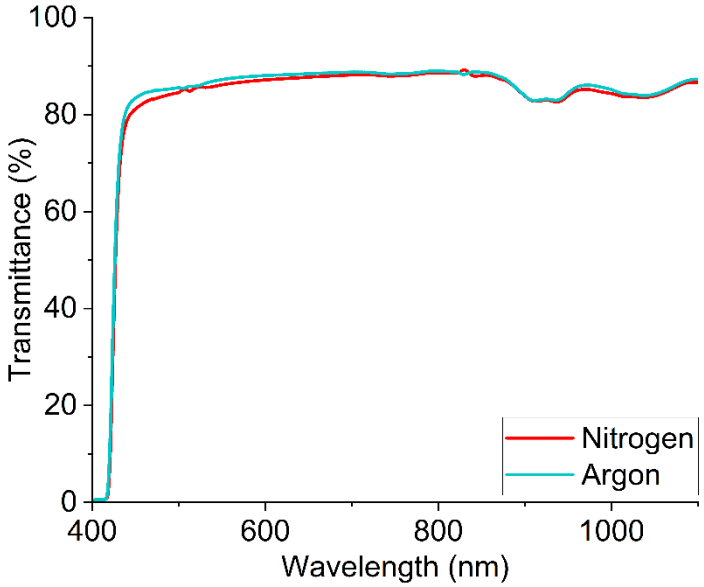

Figure S10. Transmittance spectra of a 3D printed rectangular cuboid block with **resin 1** post-cured in nitrogen (red) and argon atmosphere (light blue).

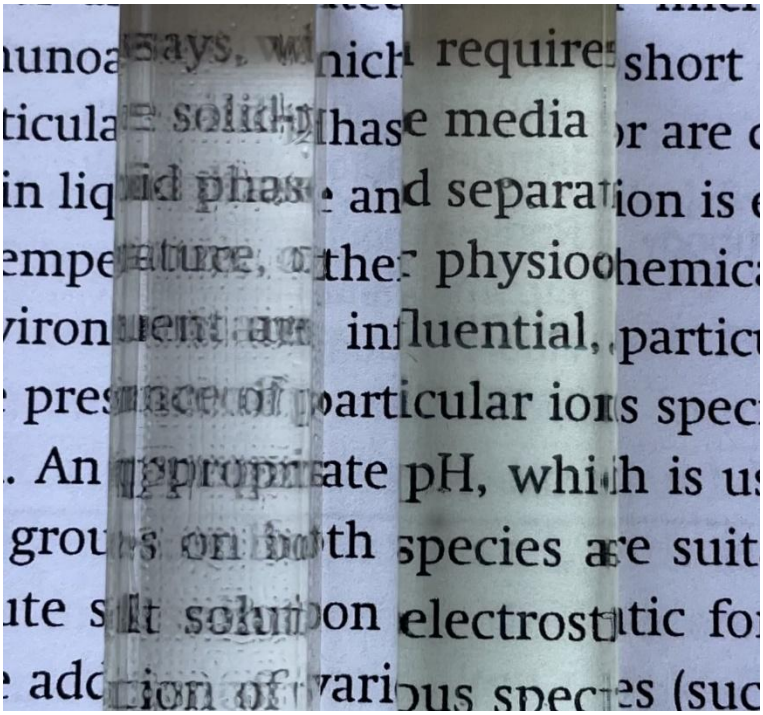

Figure S11. Two rectangular cuboid-elements prepared from **resin 2**, post-cured at 405 nm for more than 1 min, showing shrinkage (left) and post-cured at 405 nm for 30 s, yielding a smooth surface without further morphological changes (right).

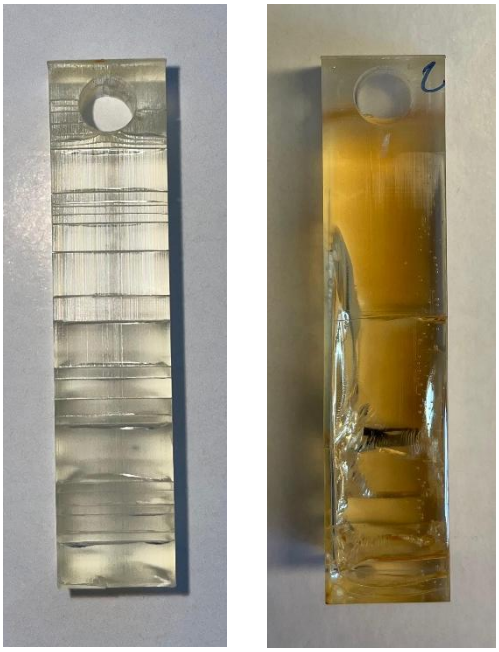

Figure S12. Two rectangular cuboid-elements prepared from **resin 1**, post-cured in the dark in an oven at 100°C for 3 h, without coating (left) and with coating (right)

IV. Front-face excitation-emission matrices

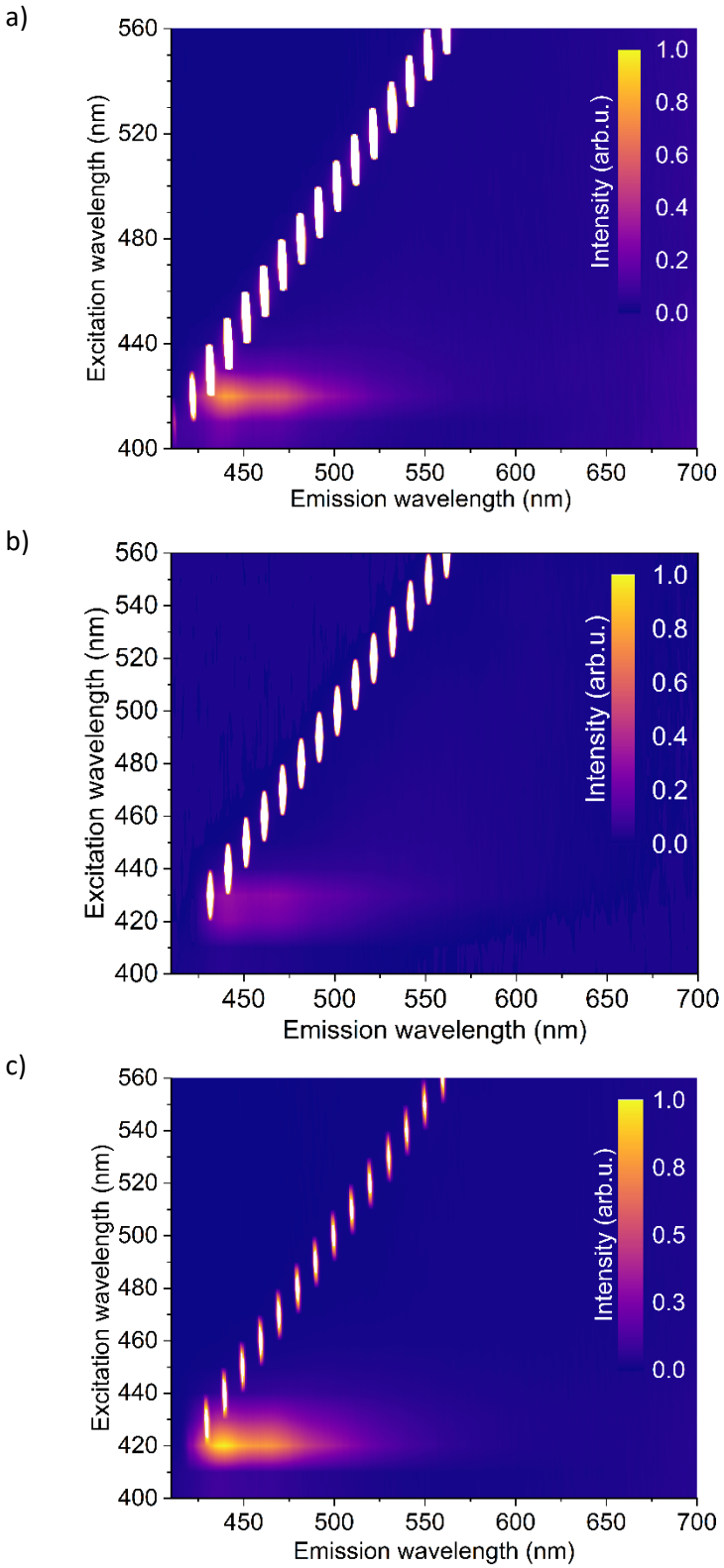

Figure S13. Front-face excitation-emission matrices of rectangular cuboid blocks from **resins 1** (a), **3** (b) and **5** (c).

V. Environmental stability

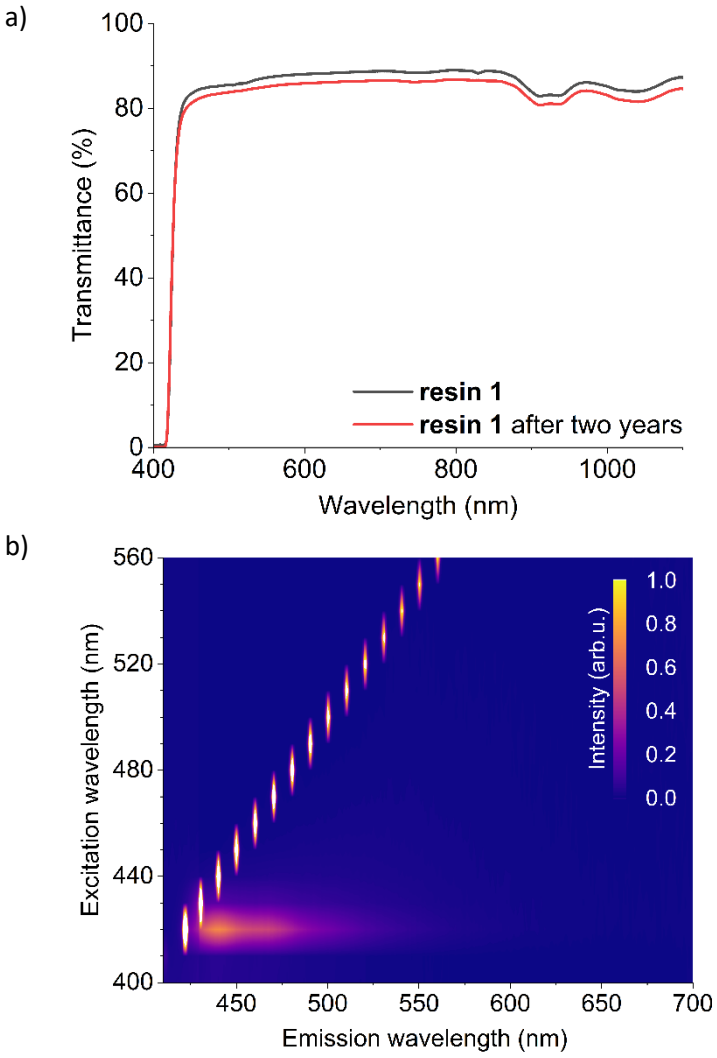

Figure S14. a) Transmittance spectra of an exemplary 3D printed rectangular cuboid block made from **resin 1** as prepared (dark) and after two years storage in the dark, at room temperature, in air (in a standard drawer of a laboratory cabinet, red). b) Corresponding front-face excitation-emission matrix (EEM) of the cuboid block after two years storage; for EEM of as-prepared block, see Figure S13a.

VI. Refractive indexes

Table S3. Refractive index of the rectangular cuboid elements obtained from five of the commercial resins after post-treatment.

Resin	*Refractive index*	
	589 nm	*498 nm*
1	1.471 ± 0.015	1.498 ± 0.050
2	1.533 ± 0.040	1.508 ± 0.043
3	1.481 ± 0.030	*n.m.*
4	1.489 ± 0.040	1.515 ± 0.039
5	1.443 ± 0.040	1.507 ± 0.011

n.m.: not measured

VII. Sensors

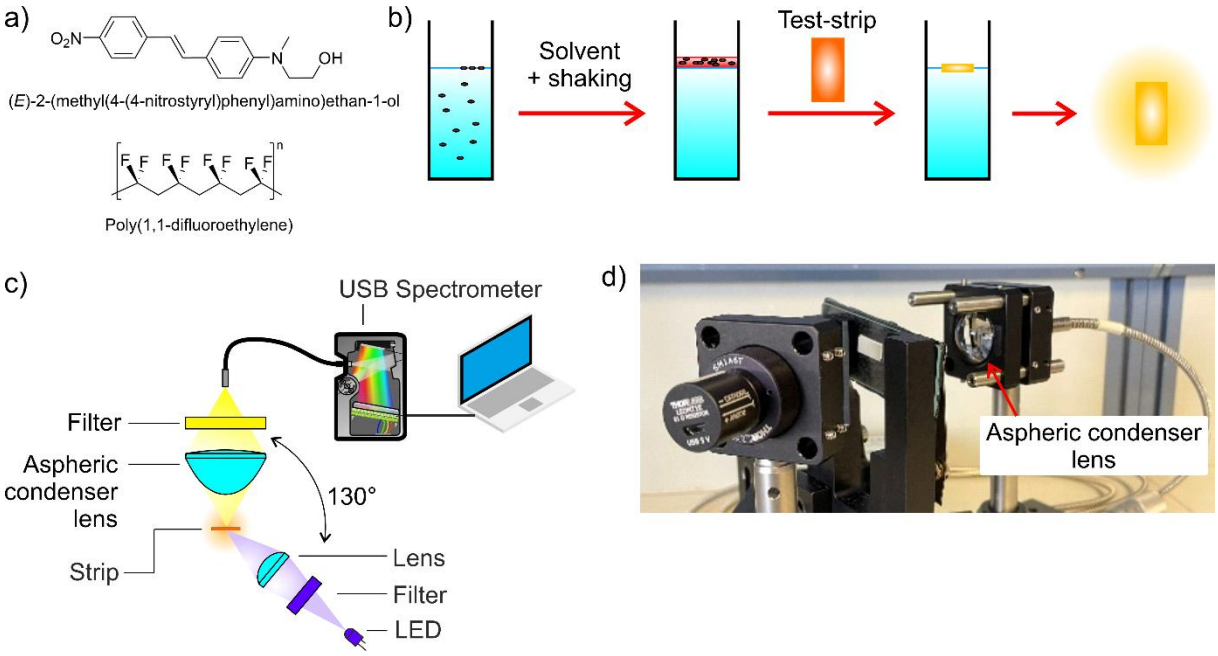

Figure S15. a) Structures of the fluorescent indicator and polymer membrane used to obtain the sensory strips. b) Protocol for sensing of total petroleum hydrocarbons in a water sample: Sampling 40 mL of water; adding 160 µL of cyclohexane as auxiliary solvent and shaking of the mixture for 1 min; placing the test strip on its surface to collect the oil; placing the strip in the readout system and recording the signal. c) Scheme of the optical setup for detecting the strip fluorescence. d) Photograph of the setup with view on the aspheric condenser lens to be exchanged between glass and resin versions of the lenses (Ø = 25.4 mm) manufactured with **resin 1**, following the method developed here, and made from NBK-7, obtained from the manufacturer (ACL25416U, Thorlabs).

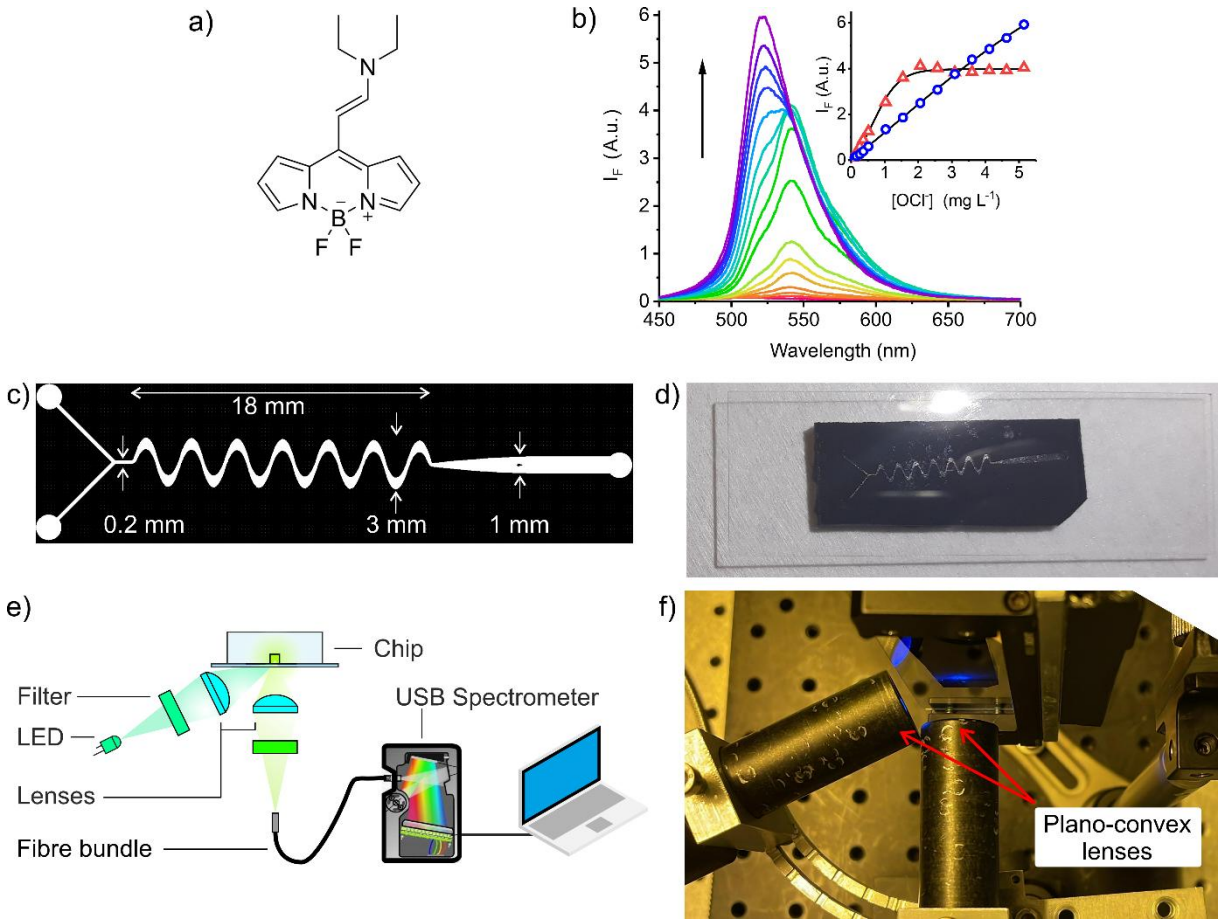

Figure S16. a) Structure of the fluorescent indicator for chlorine detection. b) Fluorescence spectra of the indicator upon increasing concentration of chlorine (NaOCl) in MeOH ($c_{indicator}$ = 10 µM, λ_{exc} = 430 nm). c) Scheme of the microfluidic chip with sinusoidal passive mixing unit for reaction of the indicator with chlorine contained in a water sample and a broader channel for fluorescence measurement. d) Photograph of the PDMS/glass chip with PDMS doped with 1 wt % of activated charcoal to obtain dark material. e) Scheme of the optical setup for detecting the indicator fluorescence modulation within the microfluidic channel. f) Photograph of the setup with positions of the plano convex lenses to be exchanged between glass and resin versions of the two small lenses (Ø = 12.7 mm) manufactured with **resin 1**, following the method developed here, and made from NBK-7, obtained from the manufacturer (LA1540, Thorlabs).

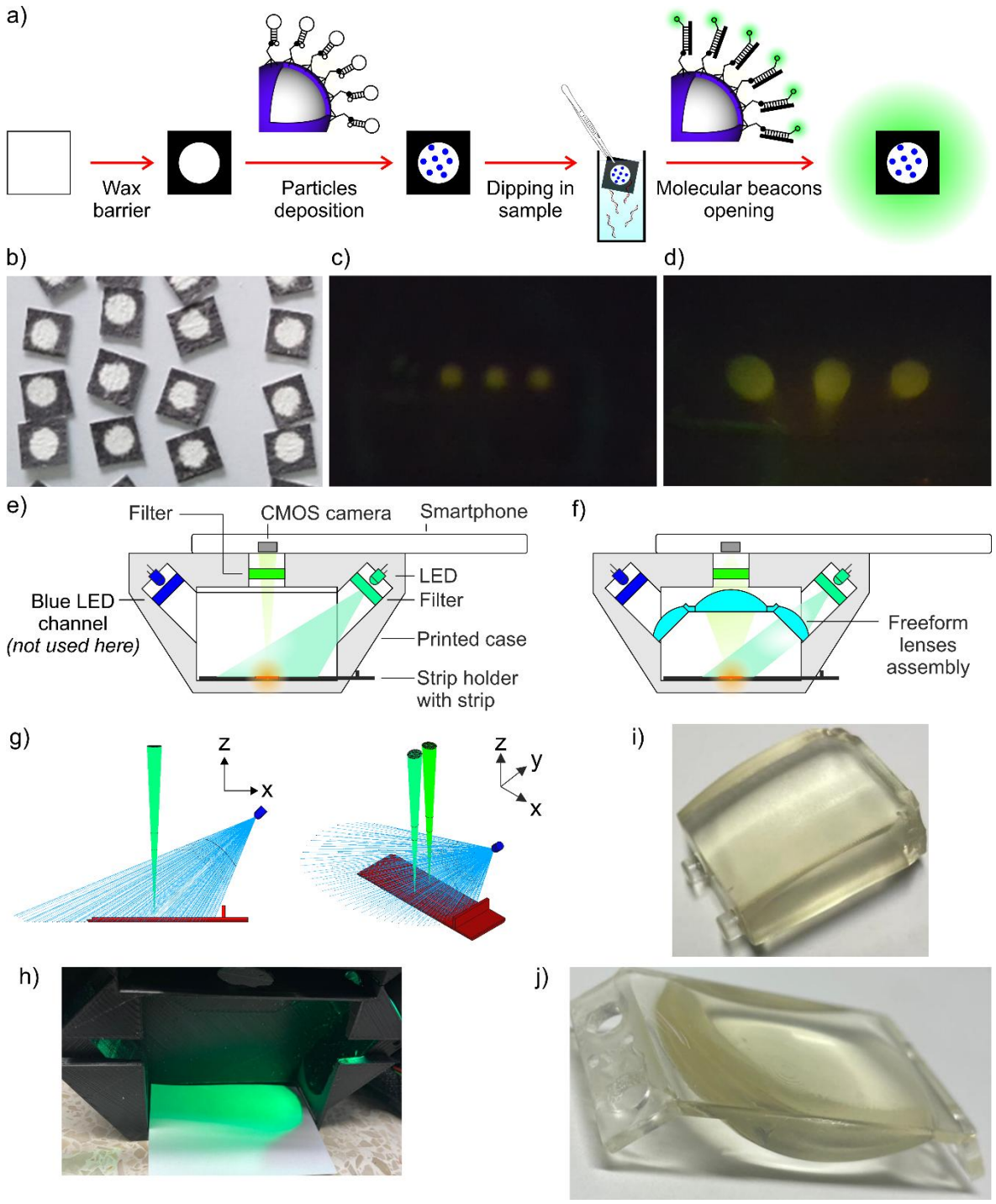

Figure S17. a) Preparation scheme of the test strip for SARS-CoV-2 sensing, including the printing of wax-barriers into a 5 × 5 mm cellulose strip, deposition of the sensory particles in the detection zone (strips can then be stored for several months at 4 °C in the dark), dipping into or deposition of the SARS-CoV-2 RNA containing sample, and placing the strip into the readout system. Photographs of b) test strips in daylight and taken with the smartphone assembly after dipping in a 10 µM solution of SARS-CoV-2 RNA c) without and d) with the free-form lenses installed in the printed case. e) Scheme of the optical assembly in the 3D printed case for smartphone read-out. f) Scheme of the assembly with insertion of the free-form optics for LED beam focusing and emission collection. (The 3D printed case comprised two excitation channels so that, for mechanical stabilisation of the lens assembly in the smartphone case, a second excitation focusing lens was required, even though the channel was not used here.) g) Ray tracing of the excitation irradiation and emission collection without the dedicated free-form optics. The sketches show the smartphone case's inner set up with excitation beam from one LED, the strip's emission, the strip holder and the 3D printed lenses (filters and 3D printed case are omitted for clarity. h) Photograph of the assembly interior without the free-form optics. Photographs of **resin 1**-made i) free-form cylindrical bi-convex lens used for LED focusing and j) truncated plano-convex lens used for emission collection (original lens: LA1385, Ø = 38.1 mm, Thorlabs).